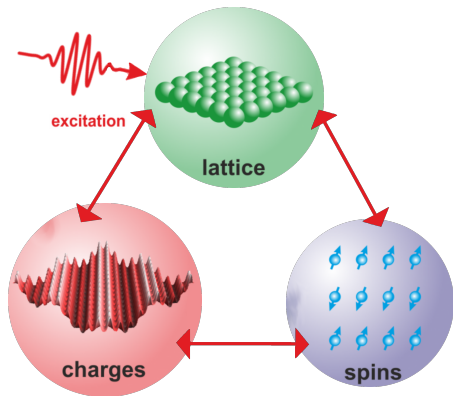
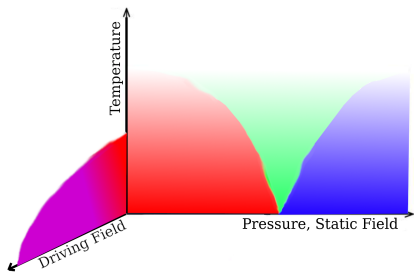


Table of Contents

- 1 Motivation
- 2 Scalable Ab-Initio Electron-Phonon Dynamics
- 3 Application
- 4 Outlook

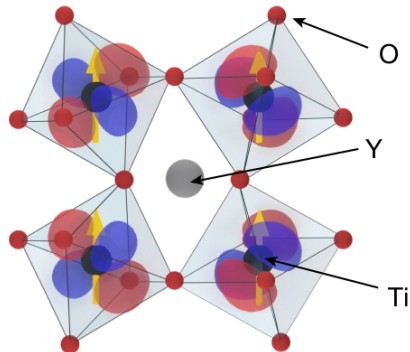
Non-Equilibrium Dynamics



Adapted from Laurenz Rettig, Fritz Haber Institute

Non-Equilibrium Dynamics: Electron-Phonon Degrees of Freedom

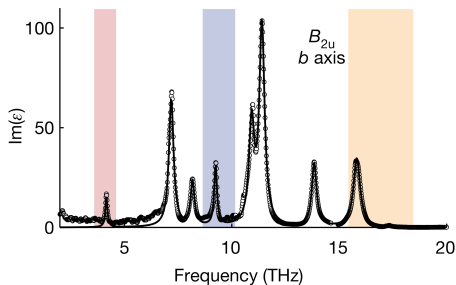
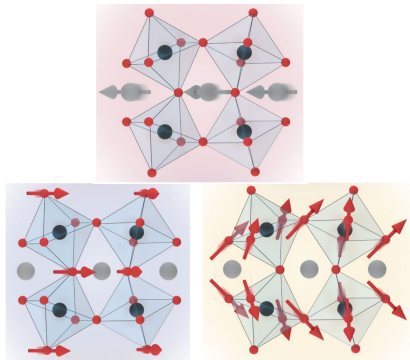
YTiO₃: Ferromagnet under 27K



Nature **617**, 73–78 (2023)

Non-Equilibrium Dynamics: Electron-Phonon Degrees of Freedom

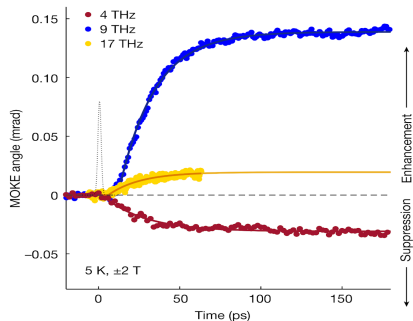
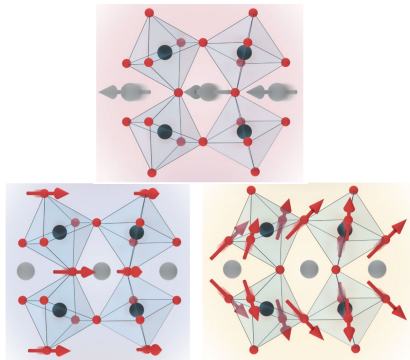
YTiO₃: Ferromagnet under 27K



Nature **617**, 73–78 (2023)

Non-Equilibrium Dynamics: Electron-Phonon Degrees of Freedom

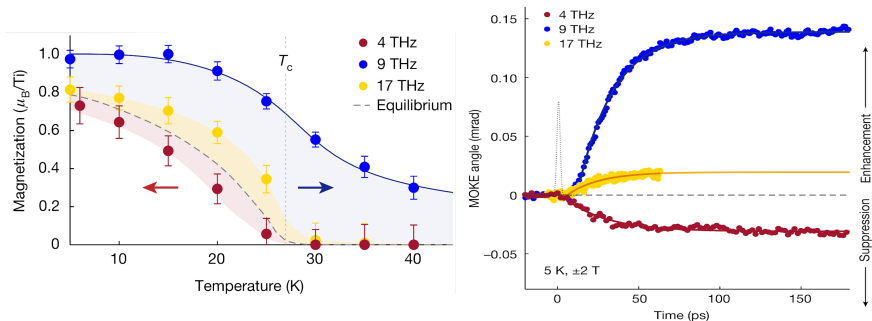
YTiO₃: Ferromagnet under 27K



Nature **617**, 73–78 (2023)

Non-Equilibrium Dynamics: Electron-Phonon Degrees of Freedom

YTiO₃: Ferromagnet under 27K

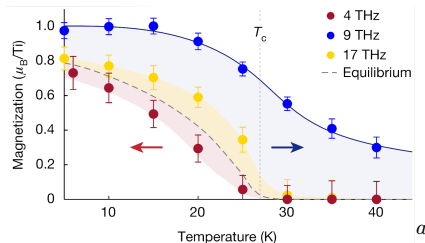


Nature **617**, 73–78 (2023)

Non-Equilibrium Dynamics: Electron-Phonon Degrees of Freedom

Explanation?

- Crystal Distortion^a
 $\sim 5 - 10\%$



^aIn similar experiments

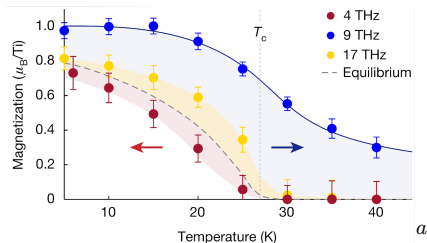
^aNature **617**, 73–78 (2023)

Non-Equilibrium Dynamics: Electron-Phonon Degrees of Freedom

Explanation?

- Crystal Distortion^a
 $\sim 5 - 10\%$
- Lattice-Orbital-Spin Interactions

^aIn similar experiments



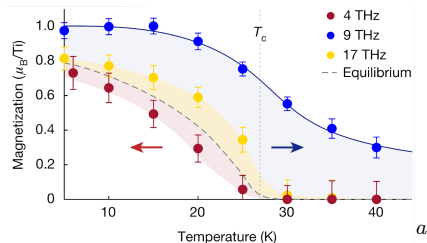
^aNature **617**, 73–78 (2023)

Non-Equilibrium Dynamics: Electron-Phonon Degrees of Freedom

Explanation?

- Crystal Distortion^a
 $\sim 5 - 10\%$
- Lattice-Orbital-Spin Interactions
- $\sim 10 - 40\text{ps} \xrightarrow{\text{relax}} \sim 1\text{ns}$

^aIn similar experiments



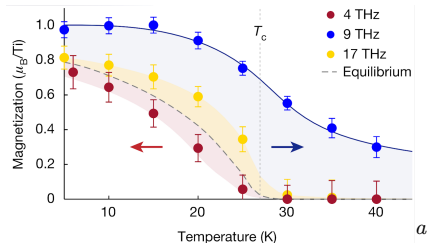
^aNature **617**, 73–78 (2023)

Non-Equilibrium Dynamics: Electron-Phonon Degrees of Freedom

Explanation?

- Crystal Distortion^a
 $\sim 5 - 10\%$
- Lattice-Orbital-Spin Interactions
- $\sim 10 - 40\text{ps} \xrightarrow{\text{relax}} \sim 1\text{ns}$
- Phenomenological Model

^aIn similar experiments



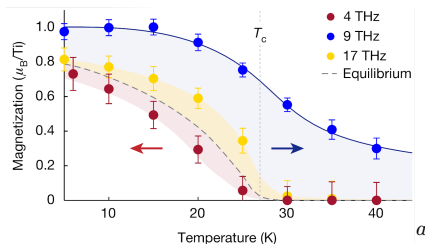
^aNature **617**, 73–78 (2023)

Non-Equilibrium Dynamics: Electron-Phonon Degrees of Freedom

Explanation?

- Crystal Distortion^a
 $\sim 5 - 10\%$
- Lattice-Orbital-Spin Interactions
- $\sim 10 - 40\text{ps} \xrightarrow{\text{relax}} \sim 1\text{ns}$
- Ab-Initio?

^aIn similar experiments

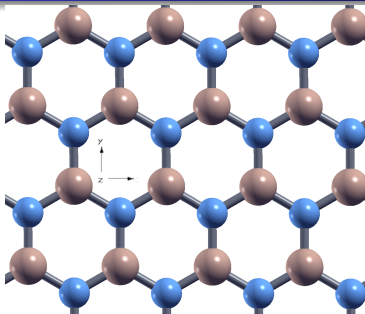


^aNature **617**, 73–78 (2023)

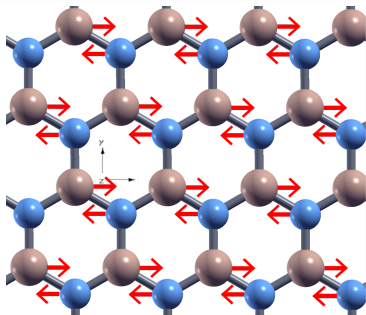
Table of Contents

- 1 Motivation
- 2 Scalable Ab-Initio Electron-Phonon Dynamics
- 3 Application
- 4 Outlook

Ab-Initio Phonon Dynamics

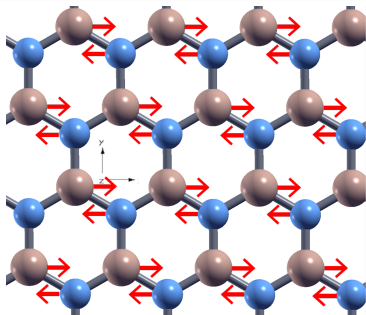


Ab-Initio Phonon Dynamics



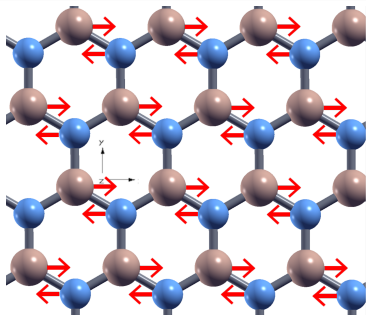
- Phonon Displacement:
 $\mathbf{e}_{\alpha\nu}(\mathbf{q}) \in \mathbb{C}^3$

Ab-Initio Phonon Dynamics



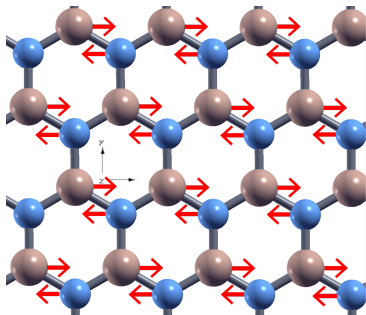
- Phonon Displacement:
 $\mathbf{e}_{\alpha\nu}(\mathbf{q}) \in \mathbb{C}^3$
- Atom α , primitive cell p

Ab-Initio Phonon Dynamics



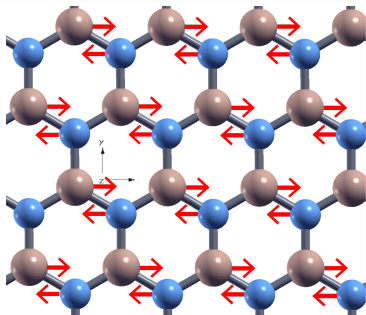
- Phonon Displacement:
 $\mathbf{e}_{\alpha\nu}(\mathbf{q}) \in \mathbb{C}^3$
- Atom α , primitive cell p
- Phonon Momenta \mathbf{q}

Ab-Initio Phonon Dynamics



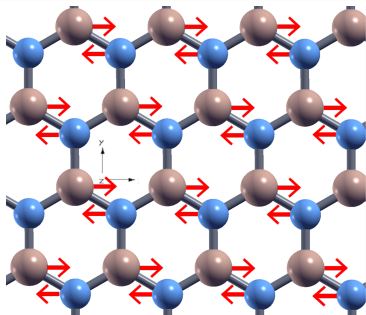
- Phonon Displacement:
 $\mathbf{e}_{\alpha\nu}(\mathbf{q}) \in \mathbb{C}^3$
- Atom α , primitive cell p
- Phonon Momenta \mathbf{q}
- Phonon Branch: ν

Ab-Initio Phonon Dynamics



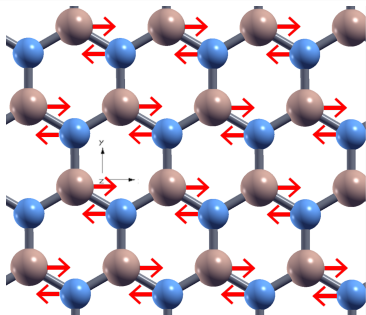
- Phonon Displacement:
 $\mathbf{e}_{\alpha\nu}(\mathbf{q}) \in \mathbb{C}^3$
- Atom α , primitive cell p
- Phonon Momenta \mathbf{q}
- Phonon Branch: ν
- Phonon Frequency: $\omega_{\mathbf{q}\nu}$

Ab-Initio Phonon Dynamics



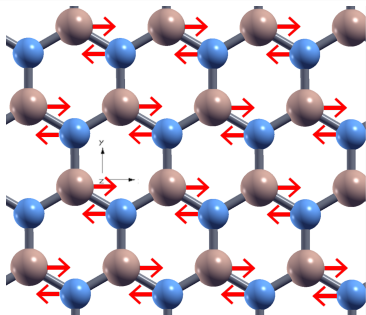
- Ionic displacement: $\delta \mathbf{R}_{\alpha p}$

Ab-Initio Phonon Dynamics



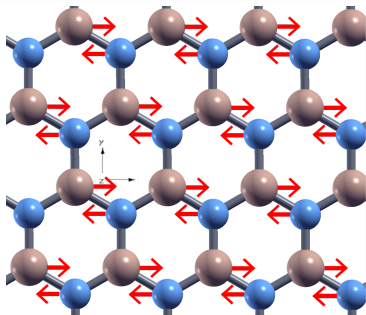
- Ionic displacement: $\delta \mathbf{R}_{\alpha p}$
- Phonon Coordinate: $z_{\mathbf{q}\nu}$

Ab-Initio Phonon Dynamics



- Ionic displacement: $\delta \mathbf{R}_{\alpha p}$
- Phonon Coordinate: $z_{\mathbf{q}\nu}$
- Phonon Momenta: $P_{\mathbf{q}\nu}$

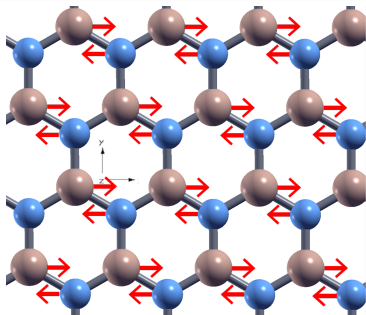
Ab-Initio Phonon Dynamics



- Ionic displacement: $\delta \mathbf{R}_{\alpha p}$
- Phonon Coordinate: $z_{\mathbf{q}\nu}$
- Phonon Momenta: $P_{\mathbf{q}\nu}$

$$\delta \mathbf{R}_{\alpha p} \propto \sum_{\mathbf{q}\nu} e^{i\mathbf{q}\cdot\mathbf{R}_p} \mathbf{e}_{\alpha\nu}(\mathbf{q}) z_{\mathbf{q}\nu}$$

Ab-Initio Phonon Dynamics

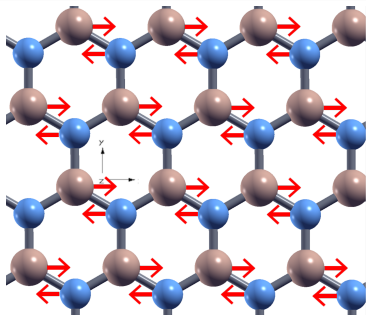


- Ionic displacement: $\delta \mathbf{R}_{\alpha p}$
- Phonon Coordinate: $z_{\mathbf{q}\nu}$
- Phonon Momenta: $P_{\mathbf{q}\nu}$

$$\delta \mathbf{R}_{\alpha p} \propto \sum_{\mathbf{q}\nu} e^{i\mathbf{q} \cdot \mathbf{R}_p} \mathbf{e}_{\alpha\nu}(\mathbf{q}) z_{\mathbf{q}\nu}$$

$$\mathbf{P}_{\alpha p} \propto \sum_{\mathbf{q}\nu} e^{i\mathbf{q} \cdot \mathbf{R}_p} \mathbf{e}_{\alpha\nu}(\mathbf{q}) P_{\mathbf{q}\nu}$$

Ab-Initio Phonon Dynamics



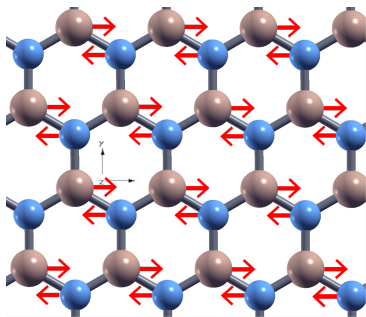
- Ionic displacement: $\delta \mathbf{R}_{\alpha p}$
- Phonon Coordinate: $z_{\mathbf{q}\nu}$
- Phonon Momenta: $P_{\mathbf{q}\nu}$

$$\delta \mathbf{R}_{\alpha p} \propto \sum_{\mathbf{q}\nu} e^{i\mathbf{q} \cdot \mathbf{R}_p} \mathbf{e}_{\alpha\nu}(\mathbf{q}) z_{\mathbf{q}\nu}$$

$$\mathbf{P}_{\alpha p} \propto \sum_{\mathbf{q}\nu} e^{i\mathbf{q} \cdot \mathbf{R}_p} \mathbf{e}_{\alpha\nu}(\mathbf{q}) P_{\mathbf{q}\nu}$$

$$\rho_{\text{ph}}^W = \prod_{\nu, \mathbf{q}} \frac{\tanh(\omega_{\mathbf{q}\nu}/2k_B T)}{\pi} \exp \left[-\tanh(\omega_{\mathbf{q}\nu}/2k_B T) \left(\tilde{z}_{\mathbf{q}\nu}^2 + \tilde{P}_{\mathbf{q}\nu}^2 \right) \right]$$

Ab-Initio Phonon Dynamics



- Ionic displacement: $\delta \mathbf{R}_{\alpha p}$
- Phonon Coordinate: $z_{\mathbf{q}\nu}$
- Phonon Momenta: $P_{\mathbf{q}\nu}$

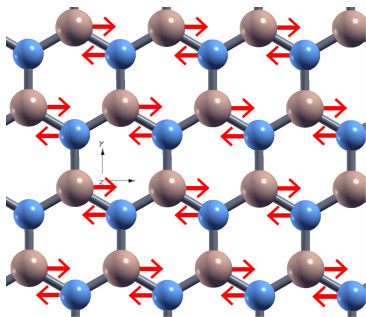
$$\delta \mathbf{R}_{\alpha p} \propto \sum_{\mathbf{q}\nu} e^{i\mathbf{q} \cdot \mathbf{R}_p} \mathbf{e}_{\alpha\nu}(\mathbf{q}) z_{\mathbf{q}\nu}$$

$$\mathbf{P}_{\alpha p} \propto \sum_{\mathbf{q}\nu} e^{i\mathbf{q} \cdot \mathbf{R}_p} \mathbf{e}_{\alpha\nu}(\mathbf{q}) P_{\mathbf{q}\nu}$$

$$\rho_{\text{ph}}^W = \prod_{\nu, \mathbf{q}} \frac{\tanh(\omega_{\mathbf{q}\nu}/2k_B T)}{\pi} \exp \left[-\tanh(\omega_{\mathbf{q}\nu}/2k_B T) \left(\tilde{z}_{\mathbf{q}\nu}^2 + \tilde{P}_{\mathbf{q}\nu}^2 \right) \right]$$

Position Identical to Existing Static Methods

Ab-Initio Phonon Dynamics



- Ionic displacement: $\delta \mathbf{R}_{\alpha p}$
- Phonon Coordinate: $z_{\mathbf{q}\nu}$
- Phonon Momenta: $P_{\mathbf{q}\nu}$

$$\delta \mathbf{R}_{\alpha p} \propto \sum_{\mathbf{q}\nu} e^{i\mathbf{q}\cdot\mathbf{R}_p} \mathbf{e}_{\alpha\nu}(\mathbf{q}) z_{\mathbf{q}\nu}$$

$$\mathbf{P}_{\alpha p} \propto \sum_{\mathbf{q}\nu} e^{i\mathbf{q}\cdot\mathbf{R}_p} \mathbf{e}_{\alpha\nu}(\mathbf{q}) P_{\mathbf{q}\nu}$$

Dynamics Not Limited to Harmonic Motion

$$\rho_{\text{ph}}^W = \prod_{\nu, \mathbf{q}} \frac{\tanh(\omega_{\mathbf{q}\nu}/2k_B T)}{\pi} \exp \left[-\tanh(\omega_{\mathbf{q}\nu}/2k_B T) \left(\tilde{z}_{\mathbf{q}\nu}^2 + \tilde{P}_{\mathbf{q}\nu}^2 \right) \right]$$

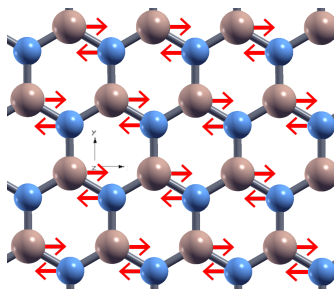
Position Identical to Existing Static Methods

Table of Contents

- 1 Motivation
- 2 Scalable Ab-Initio Electron-Phonon Dynamics
- 3 Application**
- 4 Outlook

System

hexagonal Boron Nitride (hBN)



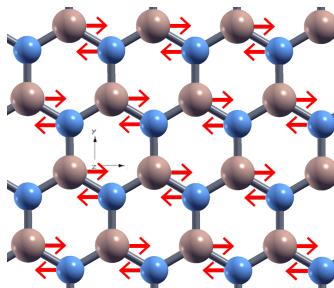
$$\tilde{z}_{\mathbf{q}\nu}, \tilde{P}_{\mathbf{q}\nu} \sim \rho_{\text{ph}}^W$$

Tight Binding (TB) Model:

$$\hat{H}_W(\mathbf{X}) = \frac{1}{2} \omega_{\mathbf{q}\nu} (\tilde{P}_{\mathbf{q}\nu}^2 + \tilde{z}_{\mathbf{q}\nu}^2)$$

System

hexagonal Boron Nitride (hBN)



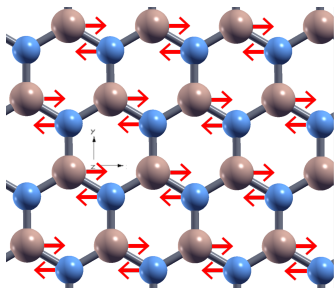
$$\tilde{z}_{\mathbf{q}\nu}, \tilde{P}_{\mathbf{q}\nu} \sim \rho_{\text{ph}}^W$$

Tight Binding (TB) Model:

$$\hat{H}_W(\mathbf{X}) = \frac{1}{2} \omega_{\mathbf{q}\nu} (\tilde{P}_{\mathbf{q}\nu}^2 + \tilde{z}_{\mathbf{q}\nu}^2) + \Delta_{\alpha} \hat{a}_{\mathbf{k}}^{\dagger} \hat{a}_{\mathbf{k}} - t_0 \left(\hat{a}_{\mathbf{k}}^{\dagger} \hat{b}_{\mathbf{k}} e^{i\mathbf{k} \cdot \boldsymbol{\delta}} + c.c. \right)$$

System

hexagonal Boron Nitride (hBN)



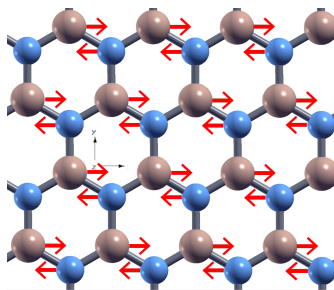
$$\tilde{z}_{\mathbf{q}\nu}, \tilde{P}_{\mathbf{q}\nu} \sim \rho_{\text{ph}}^W$$

Tight Binding (TB) Model:

$$\begin{aligned} \hat{H}_W(\mathbf{X}) = & \frac{1}{2} \omega_{\mathbf{q}\nu} (\tilde{P}_{\mathbf{q}\nu}^2 + \tilde{z}_{\mathbf{q}\nu}^2) \\ & + \Delta_\alpha \hat{a}_{\mathbf{k}}^\dagger \hat{a}_{\mathbf{k}} - t_0 \left(\hat{a}_{\mathbf{k}}^\dagger \hat{b}_{\mathbf{k}} e^{i\mathbf{k} \cdot \boldsymbol{\delta}} + c.c. \right) \\ & + \tilde{z}_{\mathbf{q}\nu} \hat{M}(\mathbf{q}, \nu, g^\nu(\mathbf{k}, \mathbf{q})) \end{aligned}$$

System

hexagonal Boron Nitride (hBN)



$$\tilde{z}_{q\nu}, \tilde{P}_{q\nu} \sim \rho_{ph}^W$$

$$\delta \mathbf{R}_{\alpha p}, \mathbf{P}_{\alpha p} \sim \tilde{z}_{q\nu}, \tilde{P}_{q\nu}$$

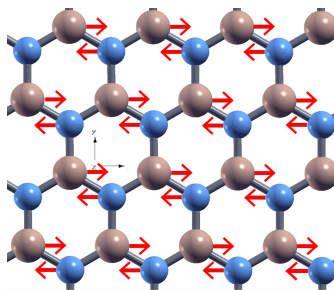
Tight Binding (TB) Model:

$$\begin{aligned} \hat{H}_W(\mathbf{X}) = & \frac{1}{2} \omega_{q\nu} (\tilde{P}_{q\nu}^2 + \tilde{z}_{q\nu}^2) \\ & + \Delta_\alpha \hat{\alpha}_k^\dagger \hat{\alpha}_k - t_0 \left(\hat{a}_k^\dagger \hat{b}_k e^{i\mathbf{k} \cdot \boldsymbol{\delta}} + c.c. \right) \\ & + \tilde{z}_{q\nu} \hat{M}(\mathbf{q}, \nu, g^\nu(\mathbf{k}, \mathbf{q})) \end{aligned}$$

TDDFT Real Space Supercells
 Real Time
 LDA xc-functional

System

hexagonal Boron Nitride (hBN)



$$\tilde{z}_{q\nu}, \tilde{P}_{q\nu} \sim \rho_{ph}^W$$

$$\delta \mathbf{R}_{\alpha p}, \mathbf{P}_{\alpha p} \sim \tilde{z}_{q\nu}, \tilde{P}_{q\nu}$$

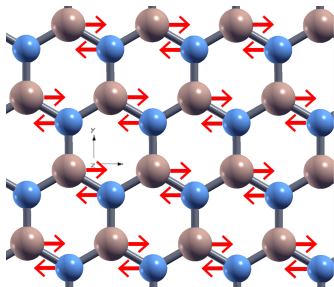
Tight Binding (TB) Model:

$$\begin{aligned} \hat{H}_W(\mathbf{X}) = & \frac{1}{2} \omega_{q\nu} (\tilde{P}_{q\nu}^2 + \tilde{z}_{q\nu}^2) \\ & + \Delta_\alpha \hat{\alpha}_k^\dagger \hat{\alpha}_k - t_0 \left(\hat{a}_k^\dagger \hat{b}_k e^{i\mathbf{k} \cdot \boldsymbol{\delta}} + c.c. \right) \\ & + \tilde{z}_{q\nu} \hat{M}(\mathbf{q}, \nu, g^\nu(\mathbf{k}, \mathbf{q})) \end{aligned}$$

TDDFT Real Space Supercells
 Real Time
 LDA xc-functional

System

hexagonal Boron Nitride (hBN)



Density Functional
 Perturbation Theory
 Input:

$$\omega_{\mathbf{q}\nu}, \mathbf{e}_{\alpha\nu}(\mathbf{q})$$

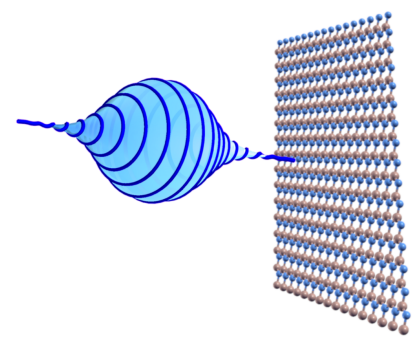
Tight Binding (TB) Model:

$$\begin{aligned} \hat{H}_W(\mathbf{X}) = & \frac{1}{2}\omega_{\mathbf{q}\nu}(\tilde{P}_{\mathbf{q}\nu}^2 + \tilde{z}_{\mathbf{q}\nu}^2) \\ & + \Delta_{\alpha}\hat{\alpha}_{\mathbf{k}}^{\dagger}\hat{\alpha}_{\mathbf{k}} - t_0 \left(\hat{a}_{\mathbf{k}}^{\dagger}\hat{b}_{\mathbf{k}}e^{i\mathbf{k}\cdot\boldsymbol{\delta}} + c.c. \right) \\ & + \tilde{z}_{\mathbf{q}\nu}\hat{M}(\mathbf{q}, \nu, g^{\nu}(\mathbf{k}, \mathbf{q})) \end{aligned}$$

TDDFT Real Space Supercells
 Real Time
 LDA xc-functional

System Dynamics

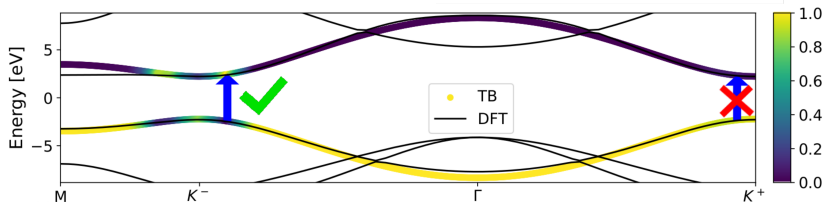
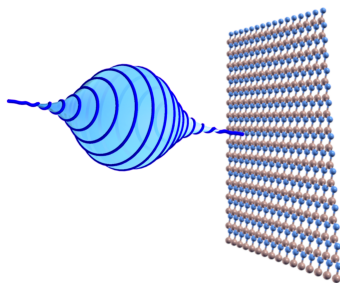
- Circularly Polarized Pump
- Ultrafast: FWHM 4.15 fs
- Intense: $7.9 \times 10^{11} \frac{\text{W}}{\text{cm}^2}$



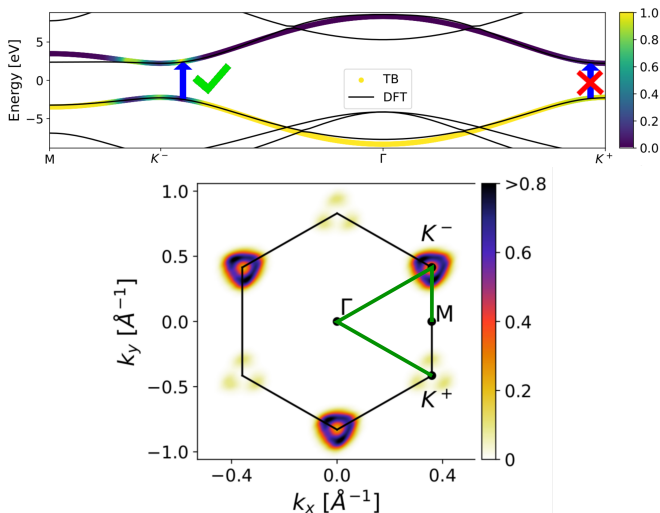
System Dynamics

- Circularly Polarized Pump
- FWHM 4.15 fs
- Only Populates one Valley

$$|c_{\mathbf{k}}|^2(t) = |\text{Tr} [\hat{\rho}(t) |n\mathbf{k}\rangle \langle n\mathbf{k}|]|^2$$

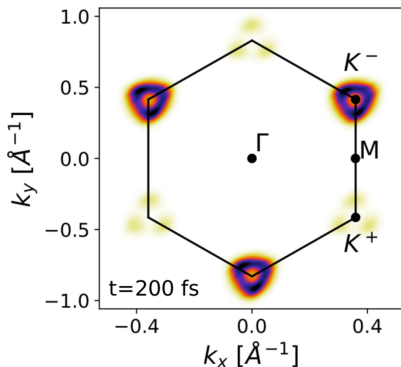


Valley Asymmetry – Theory Measure

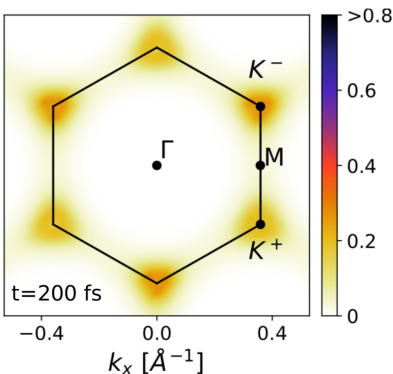


Valley Asymmetry – Theory Measure

Single Trajectory Ehrenfest

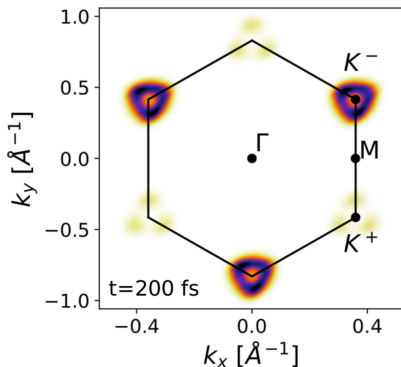


Multi Trajectory Ehrenfest

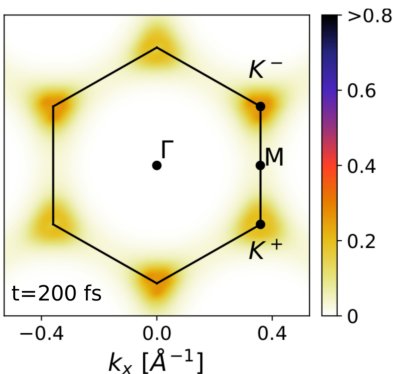


Valley Asymmetry – Theory Measure

Single Trajectory Ehrenfest



Multi Trajectory Ehrenfest



Measuring VA: Transient Circular Dichroism

Transient Absorption Spectroscopy

- Pump with Circularly Polarized Light

Measuring VA: Transient Circular Dichroism

Transient Absorption Spectroscopy

- Pump with Circularly Polarized Light
 - $\mathbf{j}_{\text{pump}}(t)$

Measuring VA: Transient Circular Dichroism

Transient Absorption Spectroscopy

- Pump with Circularly Polarized Light
 - $\mathbf{j}_{\text{pump}}(t)$
- Probe, $\mathbf{E}_{\text{probe}}$, with Circularly Polarized Light at delay τ

Measuring VA: Transient Circular Dichroism

Transient Absorption Spectroscopy

- Pump with Circularly Polarized Light
 - $\mathbf{j}_{\text{pump}}(t)$
- Probe, $\mathbf{E}_{\text{probe}}$, with Circularly Polarized Light at delay τ
 - $\mathbf{j}_{\text{pump-probe}}(t, \tau)$

Measuring VA: Transient Circular Dichroism

Transient Absorption Spectroscopy

- Pump with Circularly Polarized Light
 - $\mathbf{j}_{\text{pump}}(t)$
- Probe, $\mathbf{E}_{\text{probe}}$, with Circularly Polarized Light at delay τ
 - $\mathbf{j}_{\text{pump-probe}}(t, \tau)$

$$\mathbf{j}_{\text{TAS}}(t, \tau) = \mathbf{j}_{\text{pump-probe}}(t, \tau) - \mathbf{j}_{\text{pump}}(t)$$

Measuring VA: Transient Circular Dichroism

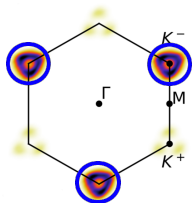
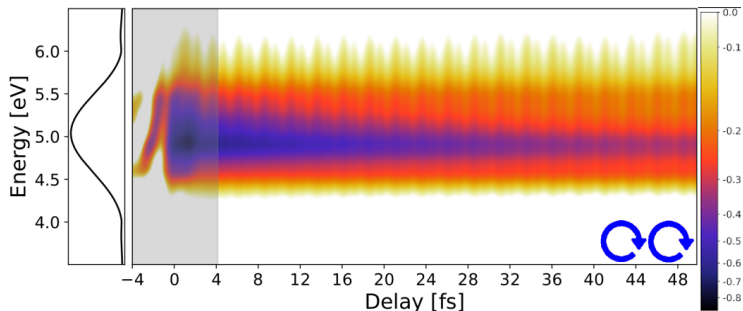
Transient Absorption Spectroscopy

- Pump with Circularly Polarized Light
 - $\mathbf{j}_{\text{pump}}(t)$
- Probe, $\mathbf{E}_{\text{probe}}$, with Circularly Polarized Light at delay τ
 - $\mathbf{j}_{\text{pump-probe}}(t, \tau)$

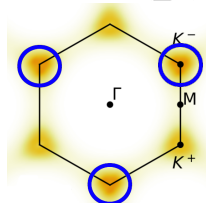
$$\mathbf{j}_{\text{TAS}}(t, \tau) = \mathbf{j}_{\text{pump-probe}}(t, \tau) - \mathbf{j}_{\text{pump}}(t)$$

$$\sigma^{\text{TAS}}(\omega, \tau) = \frac{\int dt \, j_{\text{TAS}}(t, \tau) e^{i\omega t}}{\int dt \, E_{\text{probe}}(t) e^{i\omega t}} - \sigma_{\text{equil}}(\omega)$$

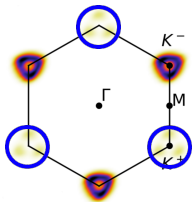
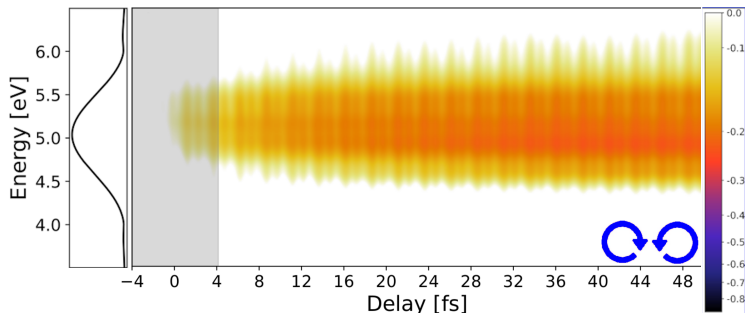
Measuring VA: Transient Circular Dichroism



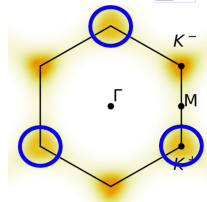
Same
 Polarization



Measuring VA: Transient Circular Dichroism

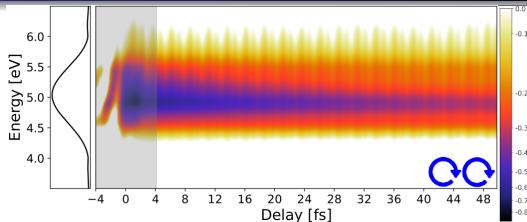


Cross
 Polarization

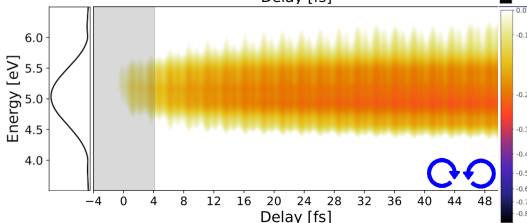


Measuring VA: Transient Circular Dichroism

$\sigma_{\text{TAS}}^{\text{same}}(\omega, \tau)$



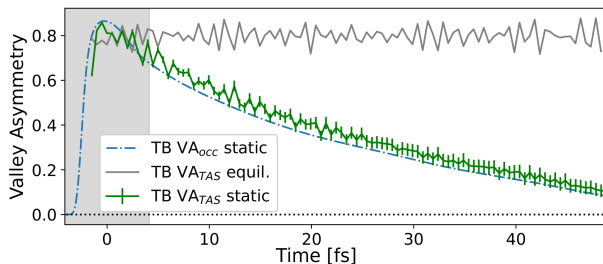
$\sigma_{\text{TAS}}^{\text{cross}}(\omega, \tau)$



$$\text{VA}_{\text{TAS}}(\tau) = \left| \frac{\int d\omega \operatorname{Re} [\sigma_{\text{TAS}}^{\text{cross}}(\omega, \tau) - \sigma_{\text{TAS}}^{\text{same}}(\omega, \tau)]}{\int d\omega \operatorname{Re} [\sigma_{\text{TAS}}^{\text{cross}} + \sigma_{\text{TAS}}^{\text{same}}(\omega, \tau)]} \right|, \quad (1)$$

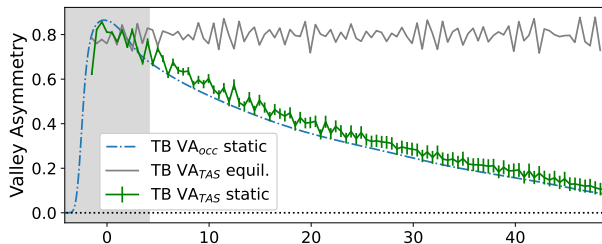
Measuring VA: Transient Circular Dichroism

TB Model

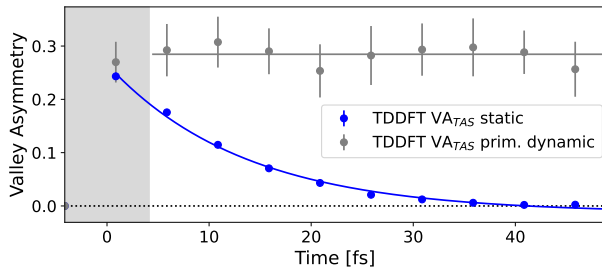


Measuring VA: Transient Circular Dichroism

TB Model



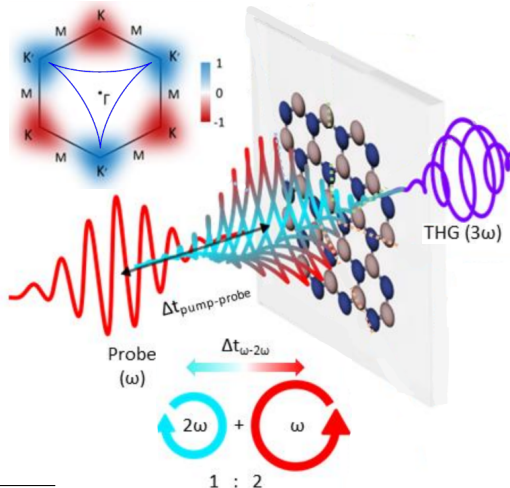
TDDFT
 1800 atoms!



Measuring VA: Harmonic Ellipticity

Highly Intense ($8 \text{ TW}/\text{cm}^2$), *off-resonant* pumping $\omega \sim 0.1 E_{\text{gap}}$

- Trefoil Pump

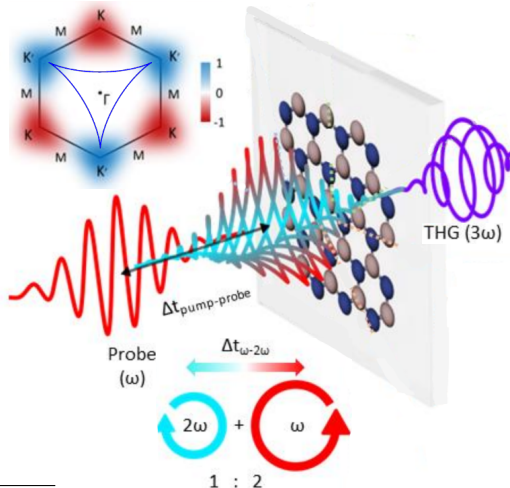


Mitra et. al Nature **628**, 752–757 (2024)

Measuring VA: Harmonic Ellipticity

Highly Intense ($8 \text{ TW}/\text{cm}^2$), *off-resonant* pumping $\omega \sim 0.1 E_{\text{gap}}$

- Trefoil Pump
- Linear Probe



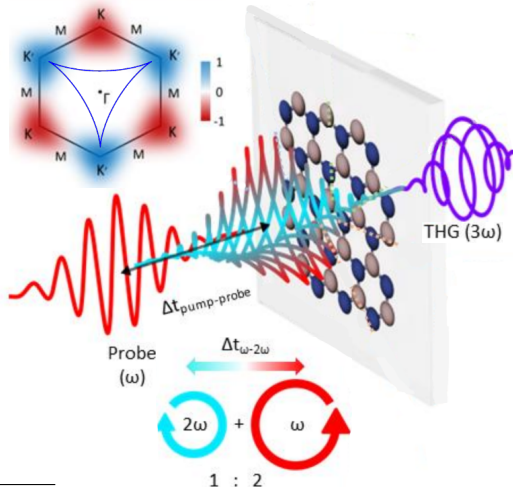
Mitra et. al Nature **628**, 752–757 (2024)

Measuring VA: Harmonic Ellipticity

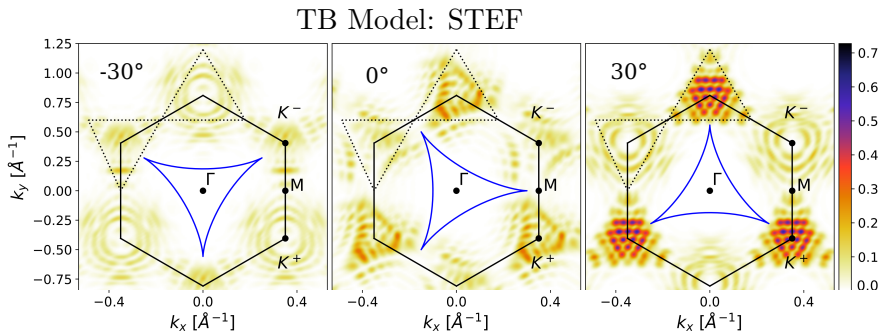
Highly Intense ($8 \text{ TW}/\text{cm}^2$), *off-resonant* pumping $\omega \sim 0.1 E_{\text{gap}}$

- Trefoil Pump
- Linear Probe

Signal from Third
 Harmonic
 Ellipticity



Measuring VA: Harmonic Ellipticity

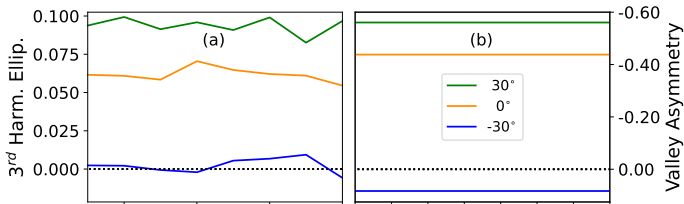


50fs after the pulse

Measuring VA: Harmonic Ellipticity

THG Ellipticity Vs. Valley Asymmetry

STEF



MTEF

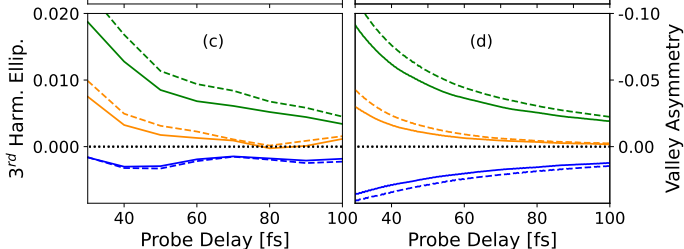


Table of Contents

- 1 Motivation
- 2 Scalable Ab-Initio Electron-Phonon Dynamics
- 3 Application
- 4 Outlook

Outlook

- Straight forward implementation across existing frameworks

Outlook

- Straight forward implementation across existing frameworks
- Arbitrary Pump Probe Simulations

Outlook

- Straight forward implementation across existing frameworks
- Arbitrary Pump Probe Simulations
- Real Time Hot Carrier Dynamics and Thermalization

Outlook

- Straight forward implementation across existing frameworks
- Arbitrary Pump Probe Simulations
- Real Time Hot Carrier Dynamics and Thermalization
 - Differential Interlayer Thermalization in Moiré Materials / Van der Waals heterostructures

Outlook

- Straight forward implementation across existing frameworks
- Arbitrary Pump Probe Simulations
- Real Time Hot Carrier Dynamics and Thermalization
 - Differential Interlayer Thermalization in Moiré Materials / Van der Waals heterostructures
 - Robustness of TAS spectra to Phonon Scattering

Outlook

- Straight forward implementation across existing frameworks
- Arbitrary Pump Probe Simulations
- Real Time Hot Carrier Dynamics and Thermalization
 - Differential Interlayer Thermalization in Moiré Materials / Van der Waals heterostructures
 - Robustness of TAS spectra to Phonon Scattering
- Dynamical/Transient Phase Transitions

Outlook

- Straight forward implementation across existing frameworks
- Arbitrary Pump Probe Simulations
- Real Time Hot Carrier Dynamics and Thermalization
 - Differential Interlayer Thermalization in Moiré Materials / Van der Waals heterostructures
 - Robustness of TAS spectra to Phonon Scattering
- Dynamical/Transient Phase Transitions
 - SrTiO₃: Paraelectric → Ferroelectric

Outlook

- Straight forward implementation across existing frameworks
- Arbitrary Pump Probe Simulations
- Real Time Hot Carrier Dynamics and Thermalization
 - Differential Interlayer Thermalization in Moiré Materials / Van der Waals heterostructures
 - Robustness of TAS spectra to Phonon Scattering
- Dynamical/Transient Phase Transitions
 - SrTiO₃: Paraelectric → Ferroelectric
 - MoTe₂: Semiconducting → Metallic phase

Outlook

- Straight forward implementation across existing frameworks
- Arbitrary Pump Probe Simulations
- Real Time Hot Carrier Dynamics and Thermalization
 - Differential Interlayer Thermalization in Moiré Materials / Van der Waals heterostructures
 - Robustness of TAS spectra to Phonon Scattering
- Dynamical/Transient Phase Transitions
 - SrTiO_3 : Paraelectric \rightarrow Ferroelectric
 - MoTe_2 : Semiconducting \rightarrow Metallic phase
 - $\text{T}_d\text{-WTe}_2$: Weyl Semimetal \rightarrow Manipulate Weyl nodes

Acknowledgements - Collaborators



Angel Rubio^{1,2}



Aaron Kelly^{1,3}



Guillermo
Albareda^{1,4}



Shunsuke A.
Sato^{1,5}

1. MPSD, Hamburg, Germany
2. Center for Computational Quantum Physics, Flatiron Institute, New York
3. Center for Ultrafast Imaging, Universität Hamburg
4. IDEADED Research, Barcelona, Spain
5. University of Tsukuba, Japan

Wigner Transform

$$\hat{O}_W(\mathbf{R}, \mathbf{P}) = (2\pi)^{-dN} \int d\mathbf{Q} e^{-i\mathbf{P} \cdot \mathbf{Q}} \langle \mathbf{R} + \mathbf{Q}/2 | \hat{O} | \mathbf{R} - \mathbf{Q}/2 \rangle$$

Ab-Initio Phonon Dynamics

Initial electron-nuclear state

Mean Field dynamics

- $|\chi\rangle \xrightarrow[\text{Transform}]{\text{Wigner}} \rho_W(\mathbf{R}, \mathbf{P})$

Kelly, A. et al, Energy Transport in Biomaterial Systems, Springer Series in Chemical Physics, 93 pp. 383-413, 2009

Ab-Initio Phonon Dynamics

Initial electron-nuclear state

Mean Field dynamics

- $|\chi\rangle \xrightarrow[\text{Transform}]{\text{Wigner}} \rho_W(\mathbf{R}, \mathbf{P})$
- $\mathbf{R}_i, \mathbf{P}_i \sim \rho_W(\mathbf{R}, \mathbf{P})$

Kelly, A. et al, Energy Transport in Biomaterial Systems, Springer Series in Chemical Physics, 93 pp. 383-413, 2009

Ab-Initio Phonon Dynamics

Initial electron-nuclear state

Mean Field dynamics

- $|\chi\rangle \xrightarrow[\text{Transform}]{\text{Wigner}} \rho_W(\mathbf{R}, \mathbf{P})$
- $\mathbf{R}_i, \mathbf{P}_i \sim \rho_W(\mathbf{R}, \mathbf{P})$
- $\hat{\rho}_e^i(\mathbf{R}_i), |\phi_i(\mathbf{R}_i)\rangle$

Kelly, A. et al, Energy Transport in Biomaterial Systems, Springer Series in Chemical Physics, 93 pp. 383-413, 2009

Ab-Initio Phonon Dynamics

Initial electron-nuclear state

- $|\chi\rangle \xrightarrow[\text{Transform}]{\text{Wigner}} \rho_W(\mathbf{R}, \mathbf{P})$
- $\mathbf{R}_i, \mathbf{P}_i \sim \rho_W(\mathbf{R}, \mathbf{P})$
- $\hat{\rho}_e^i(\mathbf{R}_i), |\phi_i(\mathbf{R}_i)\rangle$

Mean Field dynamics

- $\partial_t |\phi_i(t)\rangle = -i\hat{H}_W(\mathbf{R}_i(t)) |\phi_i(t)\rangle$

Kelly, A. et al, Energy Transport in Biomaterial Systems, Springer Series in Chemical Physics, 93 pp. 383-413, 2009

Ab-Initio Phonon Dynamics

Initial electron-nuclear state

- $|\chi\rangle \xrightarrow[\text{Transform}]{\text{Wigner}} \rho_W(\mathbf{R}, \mathbf{P})$
- $\mathbf{R}_i, \mathbf{P}_i \sim \rho_W(\mathbf{R}, \mathbf{P})$
- $\hat{\rho}_e^i(\mathbf{R}_i), |\phi_i(\mathbf{R}_i)\rangle$

Mean Field dynamics

- $\partial_t |\phi_i(t)\rangle = -i\hat{H}_W(\mathbf{R}_i(t)) |\phi_i(t)\rangle$
- $\dot{\mathbf{R}}_i = -\frac{\mathbf{P}_i}{M}$

Kelly, A. et al, Energy Transport in Biomaterial Systems, Springer Series in Chemical Physics, 93 pp. 383-413, 2009

Ab-Initio Phonon Dynamics

Initial electron-nuclear state

- $|\chi\rangle \xrightarrow[\text{Transform}]{\text{Wigner}} \rho_W(\mathbf{R}, \mathbf{P})$
- $\mathbf{R}_i, \mathbf{P}_i \sim \rho_W(\mathbf{R}, \mathbf{P})$
- $\hat{\rho}_e^i(\mathbf{R}_i), |\phi_i(\mathbf{R}_i)\rangle$

Mean Field dynamics

- $\partial_t |\phi_i(t)\rangle = -i\hat{H}_W(\mathbf{R}_i(t)) |\phi_i(t)\rangle$
- $\dot{\mathbf{R}}_i = -\frac{\mathbf{P}_i}{M}$
- $\dot{\mathbf{P}}_i = -\partial_{\mathbf{R}} \langle \phi_i(t) | \hat{H}_W(\mathbf{R}_i(t)) | \phi_i(t) \rangle$

Kelly, A. et al, Energy Transport in Biomaterial Systems, Springer Series in Chemical Physics, 93 pp. 383-413, 2009

Ab-Initio Phonon Dynamics

Initial electron-nuclear state

- $|\chi\rangle \xrightarrow[\text{Transform}]{\text{Wigner}} \rho_W(\mathbf{R}, \mathbf{P})$
- $\mathbf{R}_i, \mathbf{P}_i \sim \rho_W(\mathbf{R}, \mathbf{P})$
- $\hat{\rho}_e^i(\mathbf{R}_i), |\phi_i(\mathbf{R}_i)\rangle$

Mean Field dynamics

- $\partial_t |\phi_i(t)\rangle = -i\hat{H}_W(\mathbf{R}_i(t)) |\phi_i(t)\rangle$
- $\dot{\mathbf{R}}_i = -\frac{\mathbf{P}_i}{M}$
- $\dot{\mathbf{P}}_i =$
 $-\partial_{\mathbf{R}} \langle \phi_i(t) | \hat{H}_W(\mathbf{R}_i(t)) | \phi_i(t) \rangle$

$$\langle O(t) \rangle = \frac{1}{N} \sum_i \langle \phi_i(t) | \hat{O}_W(\mathbf{R}_i(t), \mathbf{P}_i(t)) | \phi_i(t) \rangle$$

Kelly, A. et al, Energy Transport in Biomaterial Systems, Springer Series in Chemical Physics, 93 pp. 383-413, 2009

Ab-Initio Phonon Dynamics

Initial electron-nuclear state

- $|\chi\rangle \xrightarrow[\text{Transform}]{\text{Wigner}} \rho_W(\mathbf{R}, \mathbf{P})$
- $\mathbf{R}_i, \mathbf{P}_i \sim \rho_W(\mathbf{R}, \mathbf{P})$
- $\hat{\rho}_e^i(\mathbf{R}_i), |\phi_i(\mathbf{R}_i)\rangle$

Mean Field dynamics

- $\partial_t |\phi_i(t)\rangle = -i\hat{H}_W(\mathbf{R}_i(t)) |\phi_i(t)\rangle$
- $\dot{\mathbf{R}}_i = -\frac{\mathbf{P}_i}{M}$
- $\dot{\mathbf{P}}_i =$
 $-\partial_{\mathbf{R}} \langle \phi_i(t) | \hat{H}_W(\mathbf{R}_i(t)) | \phi_i(t) \rangle$

$$\langle O(t) \rangle = \frac{1}{N} \sum_i \langle \phi_i(t) | \hat{O}_W(\mathbf{R}_i(t), \mathbf{P}_i(t)) | \phi_i(t) \rangle$$

- Same evolution as Single Trajectory Ehrenfest (STEF)

Kelly, A. et al, Energy Transport in Biomaterial Systems, Springer Series in Chemical Physics, 93 pp. 383-413, 2009

Ab-Initio Phonon Dynamics

Initial electron-nuclear state

- $|\chi\rangle \xrightarrow[\text{Transform}]{\text{Wigner}} \rho_W(\mathbf{R}, \mathbf{P})$
- $\mathbf{R}_i, \mathbf{P}_i \sim \rho_W(\mathbf{R}, \mathbf{P})$
- $\hat{\rho}_e^i(\mathbf{R}_i), |\phi_i(\mathbf{R}_i)\rangle$

Mean Field dynamics

- $\partial_t |\phi_i(t)\rangle = -i\hat{H}_W(\mathbf{R}_i(t)) |\phi_i(t)\rangle$
- $\dot{\mathbf{R}}_i = -\frac{\mathbf{P}_i}{M}$
- $\dot{\mathbf{P}}_i =$
 $-\partial_{\mathbf{R}} \langle \phi_i(t) | \hat{H}_W(\mathbf{R}_i(t)) | \phi_i(t) \rangle$

$$\langle O(t) \rangle = \frac{1}{N} \sum_i \langle \phi_i(t) | \hat{O}_W(\mathbf{R}_i(t), \mathbf{P}_i(t)) | \phi_i(t) \rangle$$

- Same evolution as Single Trajectory Ehrenfest (STEF)
- Approximate dynamic correlation \rightarrow Systematic Improvements

Kelly, A. et al, Energy Transport in Biomaterial Systems, Springer Series in Chemical Physics, 93 pp. 383-413, 2009

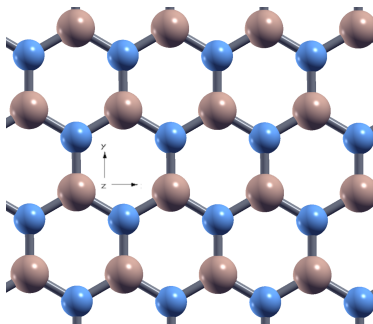
Phonon Basics

$$\begin{aligned}
 U &= U_0 + \frac{1}{2} \sum_{\alpha p, \alpha' p'} \left. \frac{\partial^2 E_0}{\partial \mathbf{R}_{\alpha p} \partial \mathbf{R}_{\alpha' p'}} \right|_{\mathbf{R}_{\alpha, p}^0, \mathbf{R}_{\alpha', p'}^0} \delta \mathbf{R}_{\alpha p} \delta \mathbf{R}_{\alpha' p'} \\
 &= U_0 + \frac{1}{2} C_{\alpha p, \alpha' p'} \delta \mathbf{R}_{\alpha p} \delta \mathbf{R}_{\alpha' p'},
 \end{aligned}$$

$$D_{\alpha, \alpha'}(\mathbf{q}) = (M_{\alpha} M_{\alpha'})^{-1/2} \sum_p C_{\alpha 0, \alpha' p} \exp(i\mathbf{q} \cdot \mathbf{R}_p),$$

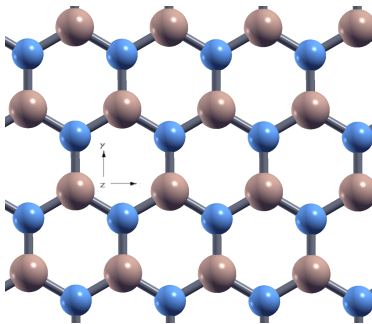
$$\sum_{\alpha'} D_{\alpha, \alpha'}(\mathbf{q}) \mathbf{e}_{\alpha' \nu}(\mathbf{q}) = \omega_{\mathbf{q} \nu}^2 \mathbf{e}_{\alpha \nu}(\mathbf{q}).$$

Electron-Phonon Dynamics



“Non-interacting” limit:

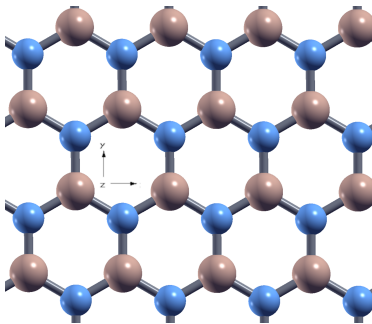
Electron-Phonon Dynamics



“Non-interacting” limit:
Equilibrium Geometry \mathbf{R}_0

$$\hat{H}(\mathbf{R}_0) |n\mathbf{k}\rangle = \epsilon_{n\mathbf{k}} |n\mathbf{k}\rangle$$

Electron-Phonon Dynamics

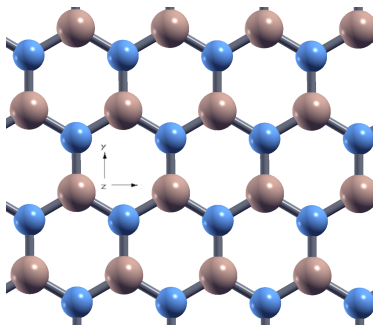


“Non-interacting” limit:
 Equilibrium Geometry \mathbf{R}_0

$$\hat{H}(\mathbf{R}_0) |n\mathbf{k}\rangle = \epsilon_{n\mathbf{k}} |n\mathbf{k}\rangle$$

$$\left(-\frac{\partial^2}{\partial \mathbf{R}^2} + \frac{\partial^2 E_0(\mathbf{R})}{\partial \mathbf{R} \partial \mathbf{R}} \Big|_{\mathbf{R}_0} \right) |n_{\mathbf{q}\nu}\rangle \rightarrow \omega_{\mathbf{q}\nu} |n_{\mathbf{q}\nu}\rangle$$

Electron-Phonon Dynamics



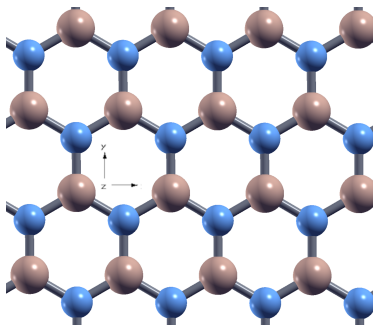
$$|n\mathbf{k}\rangle, \epsilon_{n\mathbf{k}}, |n_{\mathbf{q}\nu}\rangle, \omega_{\mathbf{q}\nu}$$

Time Dependent Boltzmann
 Equation (TDBE):

$$\partial_t |c_{n\mathbf{k}}|^2 \sim \sum_{\mathbf{q}m\nu} |g_{mn}^{\nu}(\mathbf{k}, \mathbf{q})|^2 f(|c_{m\mathbf{k}}|^2, n_{\mathbf{q}\nu})$$

$$\partial_t n_{\mathbf{q}\nu} \sim \sum_{\mathbf{k}mn} |g_{mn}^{\nu}(\mathbf{k}, \mathbf{q})|^2 h(|c_{m\mathbf{k}}|^2, n_{\mathbf{q}\nu})$$

Electron-Phonon Dynamics



$$|n\mathbf{k}\rangle, \epsilon_{n\mathbf{k}}, |n_{\mathbf{q}\nu}\rangle, \omega_{\mathbf{q}\nu}$$

Supercell Static Displacement:

Phonon Coordinates $z_{\mathbf{q}\nu} \sim \mathbf{R}$

$$O(T) = \int \frac{dz_{\mathbf{q}\nu}}{\pi \sigma_{\mathbf{q}\nu}^2(T)} e^{z_{\mathbf{q}\nu}^2 / \sigma_{\mathbf{q}\nu}^2(T)} \langle \hat{O}(z_{\mathbf{q}\nu}, T) \rangle$$

Time Dependent Boltzmann Equation

$$\begin{aligned} \partial_t f_{n\mathbf{k}} = & 2\pi \sum_{m\nu\mathbf{q}} |g_{mn}^\nu(\mathbf{k}, \mathbf{q})|^2 \\ & \times \{ (1 - f_{n\mathbf{k}}) f_{m\mathbf{k}+\mathbf{q}} \delta(\epsilon_{n\mathbf{k}} - \epsilon_{m\mathbf{k}+\mathbf{q}} + \omega_{\mathbf{q}\nu}) (n_{\mathbf{q}\nu} + 1) \\ & + (1 - f_{n\mathbf{k}}) f_{m\mathbf{k}+\mathbf{q}} \delta(\epsilon_{n\mathbf{k}} - \epsilon_{m\mathbf{k}-\mathbf{q}} - \omega_{\mathbf{q}\nu}) n_{\mathbf{q}\nu} \\ & + f_{n\mathbf{k}} (1 - f_{m\mathbf{k}+\mathbf{q}}) \delta(\epsilon_{n\mathbf{k}} - \epsilon_{m\mathbf{k}-\mathbf{q}} - \omega_{\mathbf{q}\nu}) (n_{\mathbf{q}\nu} + 1) \\ & + f_{n\mathbf{k}} (1 - f_{m\mathbf{k}+\mathbf{q}}) \delta(\epsilon_{n\mathbf{k}} - \epsilon_{m\mathbf{k}-\mathbf{q}} + \omega_{\mathbf{q}\nu}) n_{\mathbf{q}\nu} \}, \end{aligned}$$

$$\begin{aligned} \partial_t n_{\mathbf{q}\nu} = & 4\pi \sum_{mn\mathbf{k}} |g_{mn}^\nu(\mathbf{k}, \mathbf{q})|^2 f_{n\mathbf{k}} (1 - f_{m\mathbf{k}+\mathbf{q}}) \\ & \times \{ \delta(\epsilon_{n\mathbf{k}} - \epsilon_{m\mathbf{k}+\mathbf{q}} - \omega_{\mathbf{q}\nu}) (n_{\mathbf{q}\nu} + 1) \\ & - \delta(\epsilon_{n\mathbf{k}} - \epsilon_{m\mathbf{k}+\mathbf{q}} + \omega_{\mathbf{q}\nu}) n_{\mathbf{q}\nu} \}. \end{aligned}$$

MTEF Initialization

$$(\mathbf{R}_0, \mathbf{P}_0) = \mathbf{X}_0 \sim \rho_{\text{ph}}^W$$

$$\rho_{\text{ph}}^W = \prod_{\nu, \mathbf{q}} \frac{\tanh(\omega_{\mathbf{q}\nu}/2k_B T)}{\pi} \exp \left[-\tanh(\omega_{\mathbf{q}\nu}/2k_B T) \left(\tilde{z}_{\mathbf{q}\nu}^2 + \tilde{P}_{\mathbf{q}\nu}^2 \right) \right]$$

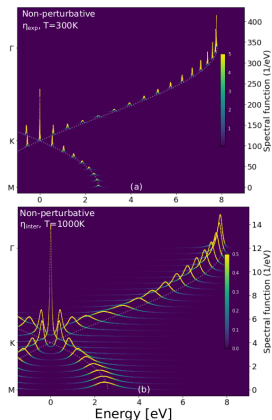
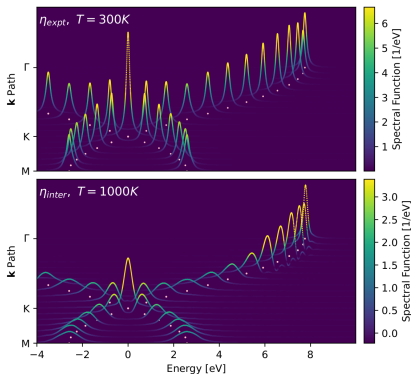
$$\hat{H}_W(\mathbf{X}^0) |\psi_l(\mathbf{X}^0)\rangle = \epsilon_l(\mathbf{X}^0) |\psi_l(\mathbf{X}^0)\rangle$$

$$\hat{\rho}_e = \sum_l f(\epsilon_l^0, T) |\psi_l\rangle \langle \psi_l|$$

Phonon Dressed Electronic Spectral Functions

$$A_{\mathbf{k}}(\omega) = \text{Im} [G_{W,n\mathbf{k}}(\omega)]$$

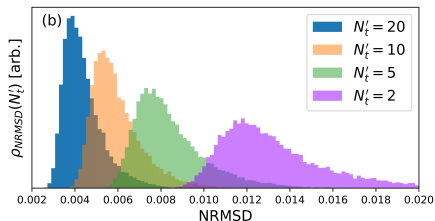
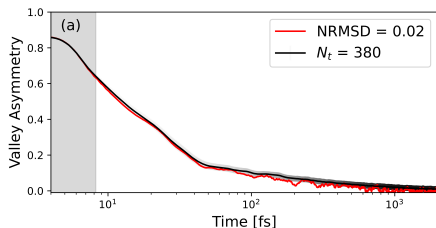
$$G_{W,n\mathbf{k}}(t) = \frac{i}{N_t} \sum_{il} \langle n\mathbf{k} | \psi_l^i(t) \rangle \langle \psi_l^i(t=0) | n\mathbf{k} \rangle$$



Phys. Rev. B **105**, 245120

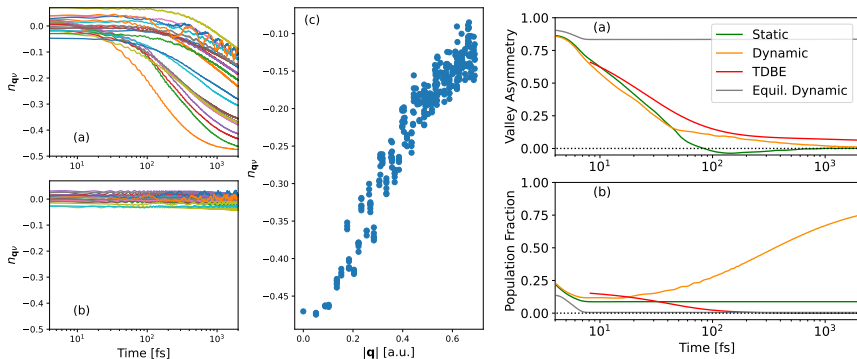
Rapidly Convergent

Distanced to Converged answer: NRMSD



$$\text{NRMSD} = \sqrt{\int_{t_i}^{t_f} dt (f(t) - g(t))^2 / (t_f - t_i) / (\max(f) - \min(f))}$$

ZPE Loss



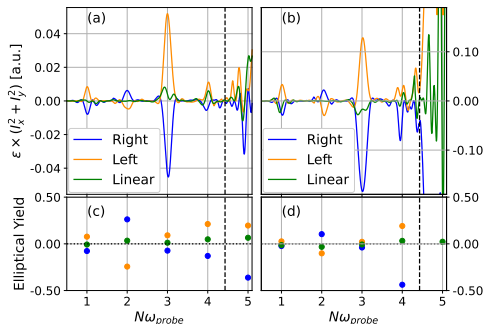
HHG Ellipticity

HHG Ellipticity Signal Picks up Valley Asymmetry

Resonant Circularly Polarized Pump

$$I_{x,y}(\omega) \propto \int dt e^{i\omega t} \partial_t j_{x,y}(t)$$

$$\epsilon [I_{x,y}(\omega)] \in [-1, 1]$$



(a): Tight Binding, (b): TDDFT